Postprint of: Lentka Ł., Smulko J., Methods of trend removal in electrochemical noise data – overview, MEASUREMENT, Vol. 131 (2019), pp. 569-581, DOI: 10.1016/j.measurement.2018.08.023

Authors:

Ł. Lentka, J. Smulko

Faculty of Electronics, Telecommunications and Informatics, Gdańsk University of Technology,

Narutowicza 11/12, 80-233 Gdańsk, Poland

Correspondence: janusz.smulko@pg.edu.pl

Title:

Methods of trend removal in electrochemical noise data – overview

Abstract:

In this paper we shall review popular methods of trend removal from electrochemical noise time records. The basic principles of operation of the six most popular methods are explained. The proposed methods are: high-pass filtering, Moving Average Removal, polynomial detrending, wavelet detrending, Empirical Mode Decomposition and Variational Mode Decomposition. Estimation of trend removal quality is evaluated using statistical measures like a histogram of noise voltage, power spectral density, the correlation coefficient and signal power. The advantages, disadvantages, limitations and applications of all of the methods mentioned are presented. Two examples of electrochemical noise data with a different nature of generation are used for assessing the efficiency of the presented methods. The first set of measurement data concerning electrochemical noise with a thermal drift were observed during uniform corrosion. The second one refers to noise superimposed on a curve of the discharging current of a supercapacitor. This additive noise component is generated by charge redistribution or redox reactions within porous carbon electrodes. A comparison of these methods and an indication of the most suitable one for removing the drift component from the acquired electrochemical data is summarized in this paper.

Keywords:

Trend removal, electrochemical noise, supercapacitors, homogenous corrosion, thermal drift.

1. Introduction

The determination of the statistical properties of a random time series is of increasing importance in various applications, beginning with the econometric data [1], biological experiments [2], quality prediction for electronic devices [3], gas sensing by low frequency resistive noise [4] or corrosion rate evaluation [5]. When time records of low-frequency noise are considered we may expect that a slowly changing trend component will interfere with that noise and that the precision of estimating its statistical parameters will deteriorate (e.g., power spectral density). Therefore, we have reason to propose an efficient method of trend removal. This issue has attracted numerous scientists and various methods have been proposed to solve it [6–8]. Any of the proposed methods may be considered as an optimal method of to remove various trends and therefore we decided to focus on that problem once again. Moreover, new materials and electrochemical charge storage media (e.g. supercapacitors,

batteries) or electricity production elements (e.g. fuel cells) require measurements of the low-frequency noise generated within their structures, and used for their characterization. Due to some unavoidable nonstationary conditions during the measurement process, an additive trend component is observed and must be removed prior to further noise data analysis.

Brockwell and Davies presented some elementary knowledge about time series analysis in their book [7]. They introduced a time series $x(t)$ model with additive components representing trend and seasonality:

$$x(t) = m_t + s_t + y(t), \tag{1}$$

where m_t is a slowly changing function called a trend component, s_t is a periodical function representing a seasonal component, and $y(t)$ is a random variable which is a noise component. The authors presented some selected methods of extracting the deterministic components m_t and s_t to identify the residual noise component $y(t)$ as a stationary time series. Alexandrov et al. [8] presented a similar model exhibiting a trend as a smooth additive component. Other authors [9–11] called that component a drift. In this paper we shall use the terms 'drift' and 'trend' interchangeably for the non-stationary component of an analysed time record.

The issue of trend removal is especially noticeable when we consider electrochemical noise data [12–14]. Electrochemical noise is usually only a very low-frequency noise within a frequency band of typically up to 1 Hz [15]. An exception to this generalization is the noise generated by e.g. turbulent processes [16]. It is time-consuming to record a sufficient number of noise samples to estimate power spectral density with an acceptable random error. During a long recording time, reaching even tens of hours, some unavoidable slow changes of temperature or other unidentified factors induce some changes (drift) in the observed current or voltage records. In general, we can reject the drift component at the data acquisition stage using high-pass (HP) filtering, but filtering would induce a relatively long lag time and is therefore impractical. Additionally, in some applications the drift component may also be useful for data analysis. Therefore, we ought to determine both components (noise and drift) separately. The quality of an applied method may be assessed using statistical measures. In our studies, we present popular trend removal methods with their benefits, disadvantages and limitations. Four frequently employed measures were used to evaluate the efficiency of the drift identification methods: probability distribution (or its estimator – histogram), power spectral density, correlation coefficient and signal power. The methods were applied to the processing of electrochemical data (i) observed during the corrosion processes and used for corrosion rate evaluation or (ii) observed during supercapacitor discharging to evaluate the 1/f-like noise intensity for its quality assessment. The analysed random time series were observed at a low frequency range when the power spectra of inherent noise of the applied measurement set-ups were at least ten times less intense than the recorded noise. The conclusions, presenting the efficiency of selected methods are given at the end of the paper.

We would like to underline that the published papers and reviews of various trend removal methods consider selected methods by presenting only examples of results obtained with the methods (e.g., HP filtering, moving-average filtering or polynomial approximation [11]; trend removal by linear function [14]; wavelet transform or empirical mode decomposition [17]). Some researchers evaluate quality of the applied methods by comparing power spectral densities of the identified noise components [18] or correlation coefficients for the signals after trend removal [17]. We claim that these ways of evaluating detrending efficiency may be limited and therefore we propose to consider using histograms of the identified noise components to evaluate efficiency of the applied detrending

methods. Our approach is possible when we record relatively long time series to estimate a histogram of the analysed signal.

This paper uses also a recently developed method of variational mode decomposition of the signal. This method may be more appropriate when the trend component is nonlinear and non-stationary due to its better capability of decomposing the signal into subbands of different widths. We will compare this method with the method based on the wavelet transform and empirical mode decomposition.

A new approach considering histogram and variational mode decomposition has never been proposed for electrochemical noise data analysis to the best of our knowledge. Additionally, we analyse the current recorded during discharging of supercapacitor to determine the additive noise component. These problems have never been presented.

2. Methods of trend removal

We have taken into account a few popular methods of trend removal and studied their efficiency for selected electrochemical signals exhibiting various drift components. Our analysis began with the high-pass filtering method which is very simple but efficient when the spectra of drift and noise components are separated.

Another method which was considered uses moving-average filtering and is quite similar to the high-pass filtering method. This method can easily be implemented and adjusted to the analysed data by modifying the cut-off filtering frequency and by smoothing the data using the method of averaging different numbers of neighbouring data samples.

The next method uses trend approximation by a polynomial. This method is well known, easily implemented and can produce reasonable results for some data. Unfortunately, this method may be far from optimal or even satisfactory for numerous time records observed during abundant experiments.

A more general method makes use of a wavelet transform. This is a type of filtering method which decomposes the analysed signal into subbands of different width and is therefore more general and efficient for trend removal than the previously mentioned methods.

Finally, we consider two recently proposed methods: empirical mode decomposition (EMD) and variational mode decomposition (VMD). These methods are more widely used for the determination of trends which have various time distributions than the above presented ones but require more advanced and time-consuming computations.

The considered methods were selected due to the applications of non-stationary random time series analysis to phenomena of relatively slow rates, requiring hours or even days of signal recording. This means that at least some of these methods should give relatively good results even if applied to a limited number of the recorded signal samples. We focused on considering efficiency of the applied method, evaluated by statistical parameters, and requirements on the number of the recorded and analysed samples. These factors determined the references considering experimental time series and next the references explaining selected methods of detrending. We should underline that the issue of trend removal, especially for electrochemical noise, continuously focuses attention of the researchers and new results were published in recent years [10, 17, 19].

2.1 High-pass filtering

In general, the operation of trend removal is high-pass (HP) filtering. At the same time a low-pass filtering (LP) may be considered as a method used to determine the trend or seasonal components (Figure 1). The filtering may apply to either digital filtering after or analogue filtering during the data acquisition process. It is possible to apply digital filtering in real time but it is more common to do this after the data acquisition process has ended [11]. When either the trend or the seasonal component is being removed during the data acquisition process there is a risk of losing information which could be potentially important.

In [11] the authors showed that HP filtering may be used to extract the trend component dominating at low frequencies. There are a large variety of digital filtering algorithms. We are not able to present an overview of all of them but we may conclude that this method is very efficient when noise and trend are situated in different bandwidths. Such a case occurs when the noise component is a random equally distributed white noise and the seasonal component is a harmonic signal (Figure 1). In that case, the operation of filtering separates both components without any problem. Unfortunately, when the trend consists of a few different components we cannot ensure that such a clear separation by an ordinary filter will occur. We have decided to limit the presentation of HP filtering methods to moving average filtering only because of the limited applications of the method to the case when noise and trend belong to two different bandwidths as well as problems of selecting the most efficient filter from a great variety of HP filters.

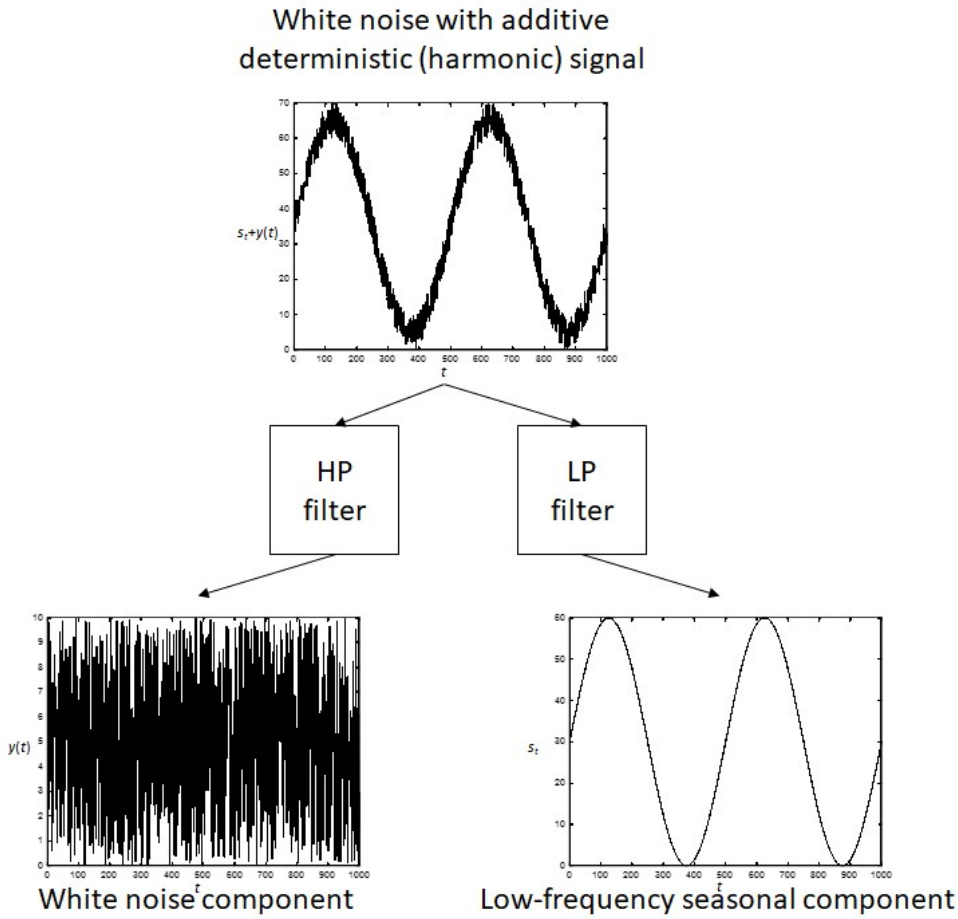

Figure 1. Illustration of removal of the seasonal component or its extraction by high-pass (HP) and low-pass (LP) filtering, respectively.

2.2 Moving Average filtering

The Moving Average method is used for smoothing the recorded random data, giving similar results as observed in the case of LP filtration. It creates a series of averages of selected subsets from the full data set. However, thanks to the introduction of only a small change in this procedure we may obtain the moving average removal (MAR), which is a type of HP filtration. The MAR method for the analysis of the electrochemical noise was first proposed by Tan et al. [13]. The formula for an output value y_n of the MAR filter is as follows:

$$y_n = x_n - m_n, \tag{2}$$

$$m_n = \frac{1}{2p+1}(x_{n-p} + \cdots + x_{n-1} + x_n + x_{n+1} + \cdots + x_{n+p}), \tag{3}$$

where x_n denotes the n-th sample of the acquired signal at a sampling frequency f_s, m_n is a result of applying the moving average procedure to a segment starting from the point n-p to the point n+p (i.e., to a set of 2p+1 samples situated around the index n). The MAR filtering procedure may easily be implemented in any programming language (e.g., MATLAB software). That filtering process may be described by its transfer function $H(f)$ determining the relationship between the Fourier transforms of the input $X(f)$ and output $Y(f)$ signals, and is described by the formula:

$$H(f) = \frac{Y(f)}{X(f)} = 1 - \frac{1}{2p+1}\frac{\sin\left[\frac{(2p+1)\pi f}{f_s}\right]}{\sin\left(\frac{\pi f}{f_s}\right)}. \tag{4}$$

The averaging is symmetrical around the index n of the sample subset. Thus, the number of averaged samples is odd. Therefore, MAR filtering does not introduce any phase shift. Figure 2 presents a set of transfer functions $H(f)$ of an MAR filter versus the frequency for the selected values of parameter p. A greater value of p means averaging over longer subsets of the recorded samples and - therefore – extending the frequency bandwidth by a range of lower frequencies. The parameter p determines the passband of the MAR filter starting from frequency $f_s/(2p+1)$. Additionally, some ripples are introduced into the passband area (Figure 2).

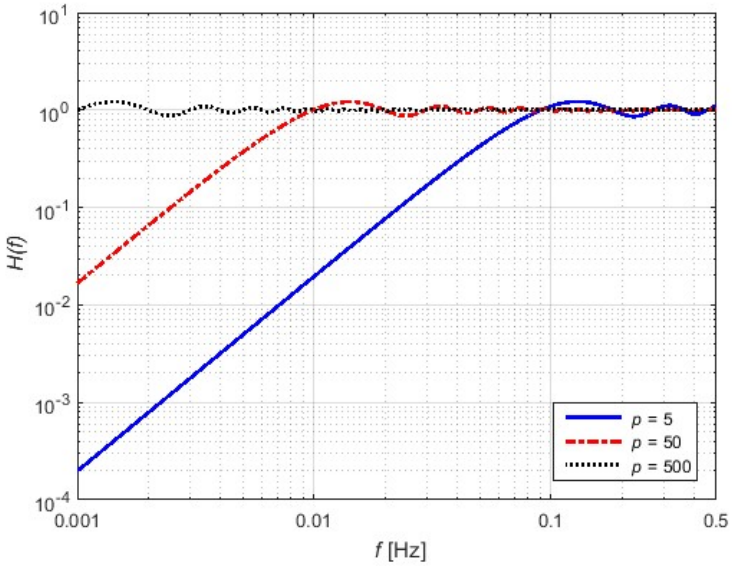

Figure 2. A set of moving average removal (MAR) filter transfer functions $H(f)$ versus normalized frequency f/f_s for selected values of the number 2p+1 of averaged samples.

The MAR filter is computationally very attractive due to its simplicity but it has some serious limitations. It effectively removes the drift, but it also removes a large part of any low-frequency components of the useful signal, crucial to an analysis of the electrochemical noise data, when their bandwidths overlap. The second limitation causes the inapplicability of the higher-order MAR filter to nonlinearly drifting signals, a characteristic feature of electrochemical noise data [11]. The MAR filter introduces artifacts into the detrended curve (when p is too high) and an unacceptable degree of filtration due to the overly high cut-off frequency (when p is too low). Numerous authors have presented the weaknesses of MAR filtering when applied to their experimental results [11, 14].

2.3 Trend removal by polynomial approximation

Polynomial detrending is another method of HP filtering commonly used for trend removal [11]. In general, it involves the approximation of the trend by a polynomial of a given order p_o. The approximated trend is fitted to the analysed time record. The polynomial is subtracted from the acquired data x_n to determine the signal y_n after detrending:

$$y_n = x_n - \sum_{i=0}^{p_o} a_i n^i, \tag{5}$$

where a_i is the i-th coefficient of the trend approximating the polynomial evaluated for a discrete time n. It is evident that for a trend of a linear function the polynomial order equals to one. A technique determining the trend $m_n = \sum_{i=0}^{p_o} a_i n^i$ present in the analysed data x_n uses the least squares criterion [7] given by the formula:

$$\min \sum_{n=1}^{N} (x_n - m_n)^2. \tag{6}$$

The evaluated coefficients a_i of the polynomial should minimize the criterion (6). This method of curve fitting is called the least squares regression and can be carried out by the MATLAB function *polyfit*.

The presented method of trend removal has some limitations. When a large number of the recorded samples are analysed a further increase of the polynomial degree does not improve the approximation but results in an overfitting effect – high-order polynomials can oscillate between consecutive samples, resulting in worse data fitting. In that case, a low-order fitting polynomial, which tends to be smoother between the points, should be used. The polynomials are unbounded, oscillatory functions and therefore they are not well-suited to extrapolating bounded or monotonic data. Depending on the complexity of the least squares regression algorithms there are different methods of evaluating polynomial coefficients (i.e., LU decomposition, QR decomposition, Givens Rotations, Housholder Transformations [20], Principal Component Regression (PCR) [21, 22] and Least Squares Support Vector Regression (LS-SVR) [9, 23]).

In [11] the authors demonstrated that the lowest frequencies could be drastically attenuated depending on the order of the polynomial – a higher order means better attenuation. The main disadvantage of the polynomial detrending method is a user-defined parameter – the polynomial order. It is selected arbitrarily and has an enormous impact on the efficiency of the method [15]. In [24] the author presents a comprehensive analysis of the polynomial's degree influence on the detrending results. The accuracy of detrending by the polynomial approximation for signals with an intense noise component decreases with the polynomial degree. When a signal is dominated by the trend component, a greater polynomial degree improves the result of the trend removal [24]. Unfortunately, it is very difficult to automatically select an optimal polynomial degree. Thus, in general, that method is usually far from being optimal but it may be relatively easy to implement.

2.4 Filtering by wavelet transform

The trend removal or trend determination based on the wavelet transform is a popular method which produces relatively good results [8, 15, 25]. The Discrete Wavelet Transform (DWT) proposed by Mallat in 1989 [26] consists of decomposing a discrete signal into a collection of band-limited low- and high-frequency components. The low-frequency components are called approximations (A) and the high-frequency components are called details (D). Figure 3 presents a block diagram of the DWT algorithm proposed by Mallat for decomposing (Figure 3a) into subbands or reconstructing (Figure 3b) the analysed signal from these subbands.

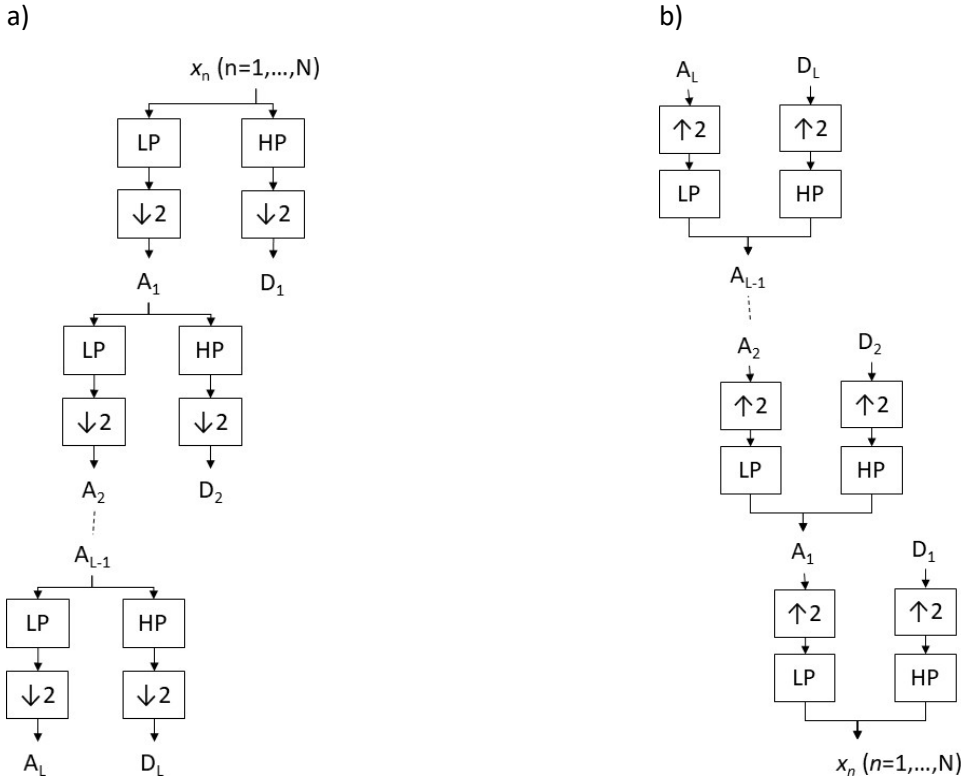

Figure 3. A block diagram of a discrete signal x_n: a) decomposed using the DWT Mallat algorithm, b) reconstructed using DWT filter banks. The operations ↓2 and ↑2 mean downsampling (removing every second sample) and upsampling (adding zero between each consecutive samples), respectively.

Signal decomposition at each stage necessitates filtering the signal independently using two digital filters. The first one is a low-pass filter (LP) and the output signal is a named approximation. The second one is a high-pass filter (HP) and the output is called detail. The outputs of both filters are downsampled – every second sample is removed (Figure 3a). Hence, a frequency band of each component equals half of the frequency band of the input signal. Therefore, a broadband input signal is decomposed into a set of approximations and details successively more limited in frequency bands. In fact, we obtain logarithmically decreasing frequency intervals and the spectra lines on a logarithmic scale are in equidistant steps [27]. The decomposed signal may be modified before reconstruction (Figure 3b) by zeroing the selected subbands. By using statistical parameters we can identify which of the details or approximations represent the noise or trend components. This procedure may be performed automatically by estimating e.g. the standard deviation and signal thresholding [28] and therefore is very attractive for practical applications (a threshold value depends on the estimated standard deviation). Another indisputable benefit of that method is its accessibility in MATLAB

software, from the *Wavelet Toolbox* [29]. The effectiveness of the presented method depends on the applied orthogonal wavelet functions. Among the most popular orthogonal wavelet functions are the Daubechies and symlet ones. In the literature [27] we can find a more detailed description of the orthogonal and dual functions commonly used in the DWT. In the class of orthogonal functions [33], there are Chebyshev's discrete polynomials. Chebyshev's discrete spectroscopy [30, 31] is resistant in respect of a drift of electrochemical noise.

The number of levels that a signal x_n is decomposed to by the DWT is determined by the sampling frequency and the bandwidth of the signal (its recording time) [26]. This number, as well as the wavelet function have to be established arbitrarily [8]. This means that the presented method, even if very attractive and effective in determining the trend component, has some drawbacks. In [14] the authors have shown a more sophisticated use of the DWT algorithm for signal detrending. They assumed that the trend component is not limited to the last approximation component, but is also partially included in some details. Moreover, they applied a modified method of soft thresholding and considered the presence of a nonwhite noise component. The results were promising and could be evaluated automatically and therefore the method is very attractive.

2.5 Empirical Mode Decomposition

The Empirical Mode Decomposition (EMD) is a method of signal analysis proposed by Huang in 1998 [32]. During EMD analysis, a signal in the time domain occurs, unlike other presented methods (e.g., the Fourier transform or the wavelet transform). In contrast to the wavelet decomposition, where data are expanded into wavelet crystals on the basis of predefined wavelet functions and using their orthogonality, the basis of EMD is derived directly from the data itself. Thus, the EMD should be more flexible and adaptive to the analysed signal than the previously mentioned methods [15]. The encouraging results of using the EMD method for trend removal were presented elsewhere [33, 34]. The analysed time record $x(t)$ was decomposed into finite additive oscillatory components called intrinsic mode functions (IMFs). An IMF has to satisfy the following two conditions:

1. the numbers of extremes and zero crossings of the signal must be either equal or different at most by one only,
2. the average values of the envelopes interpolating local maxima and interpolating local minima are equal to zero.

Figure 4 presents a block diagram of the EMD algorithm of a signal $x(t)$. In the first iteration ($j = 1$) the acquired signal with the trend component is treated as a residual $r_0(t)$ and its local extremes are determined. In the next step local maxima and minima should be interpolated using the spline function to create the upper $e_u(t)$ and lower $e_l(t)$ envelopes, respectively. Then we calculate the local average $m_1(t) = (e_u(t) + e_l(t))/2$ and the function $h_1(t) = x(t) - m_1(t)$, which is a candidate for the first IMF. If $h_1(t)$ satisfies both conditions for an IMF, we assume that it is an IMF component. If not, we take it as a signal to be analysed and repeat this procedure until it satisfies both conditions for an IMF.

Once we determined the first IMF component, we subtract it from the signal $x(t)$ and obtain a residual signal $r_1(t) = x(t) - h_1(t)$, which is now treated as the input signal. That procedure is repeated n times and the following IMF components are obtained: $h_1(t) = x(t) - r_1(t)$; $h_2(t) = r_1(t) - r_2(t)$; … ; $h_n(t) = r_{n-1}(t) - r_n(t)$. The decomposition stops when $r_j(t) = r_n(t)$ (Figure 4) is either a monotonic or constant function, which means that we are not able to extract more IMF components satisfying both conditions

mentioned above. The original signal $x(t)$ may be reconstructed by summing up all IMF components and the last residue:

$$x(t) = \sum_{j=1}^{n} h_j(t) + r_n(t). \tag{7}$$

If an EMD input signal $x(t)$ consists of a high-frequency random component $y(t)$ (noise) and a slowly changing trend component, we expect that the trend will be identified by a few IMF components $h_j(t)$ of a sufficiently large index j and the final residual.

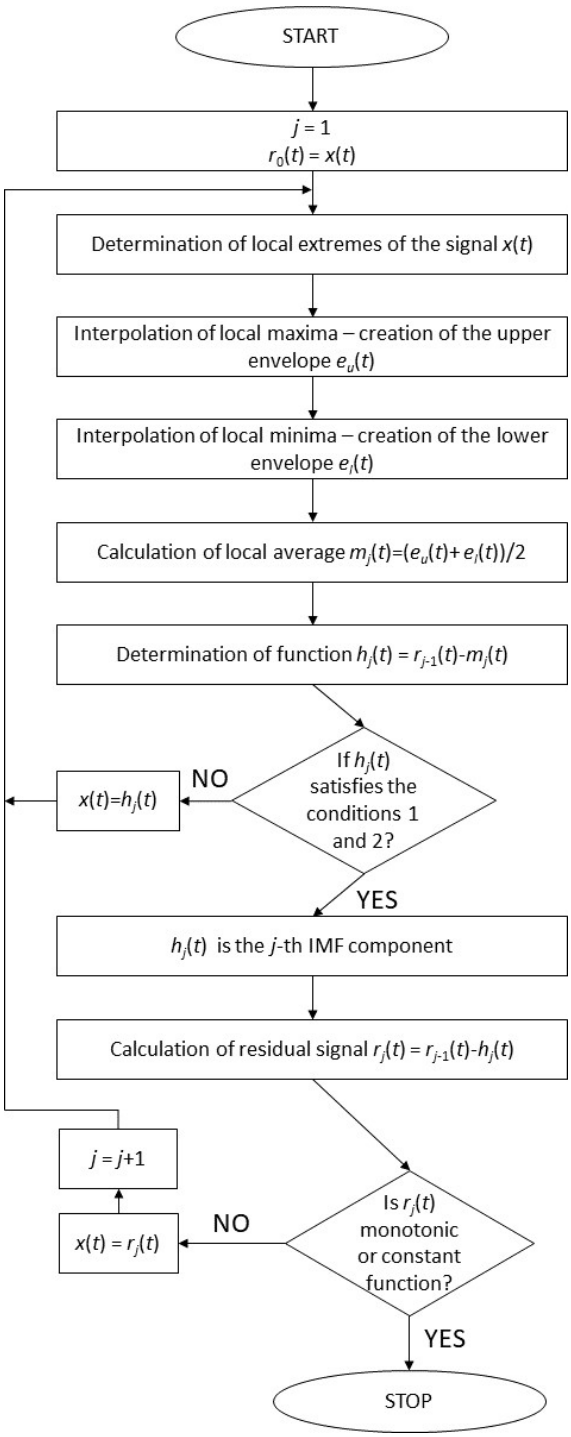

Figure 4. A block diagram of the empirical mode decomposition (EMD) algorithm.

The EMD decomposition introduced above, was successfully used to remove the trend in some examples of signal analysis [34]. The task of trend removal means the estimation of a signal random component by the formula:

$$\hat{y}_D(t) = \sum_{j=1}^{D} h_j(t), \tag{8}$$

where: $\hat{y}_D(t)$ - an estimated detrended signal $y(t)$ using the first D successive IMF components, $h_j(t)$ – the j-th IMF function, D – the largest IMF index representing the noise component. The number D may be determined by observing the evolution of the standardized empirical mean of the estimated function $\hat{y}_D(t)$ as a function of different values of D, to identify the lowest D value when the mean value of $\hat{y}_D(t)$ is significantly different from zero [34].

In [36] the authors presented a more advanced version of the trend extraction method based on the EMD algorithm. They proposed to determine the number of IMF components by evaluating how distant two consecutive IMFs were from one another when represented by the Hilbert marginal spectrum. The results were very promising for the analysed experimental data of rail corrugation measurements [36]. In [35] the authors proposed three different ways for selecting the D value: the ratio approach, the energy approach and the energy-ratio approach. The first one is based on the ratio R^i of the numbers of zero crossings of two successive (e.g. i-1 and i) IMF components and on the selection of the D value by choosing the smallest index i for which R^i is significantly different from 2. The second approach is based on the energy estimation G^i of all evaluated IMF components and then on finding such an index $i = D$ ($i \geq 2$) for which the energy estimations of two successive IMFs are related: $G^i > G^{i-1}$. The last approach is based on a combination of the two previously mentioned approaches, and is capable of reducing the number of false detections. It assumes that D is the smallest common index i in both previous approaches.

The EMD method can easily be implemented in MATLAB software or in C language. There is a ready-to-use MATLAB code using that method [33, 34]. Some examples of the results of the EMD algorithm decomposing a signal with the trend component are presented in Figure 5.

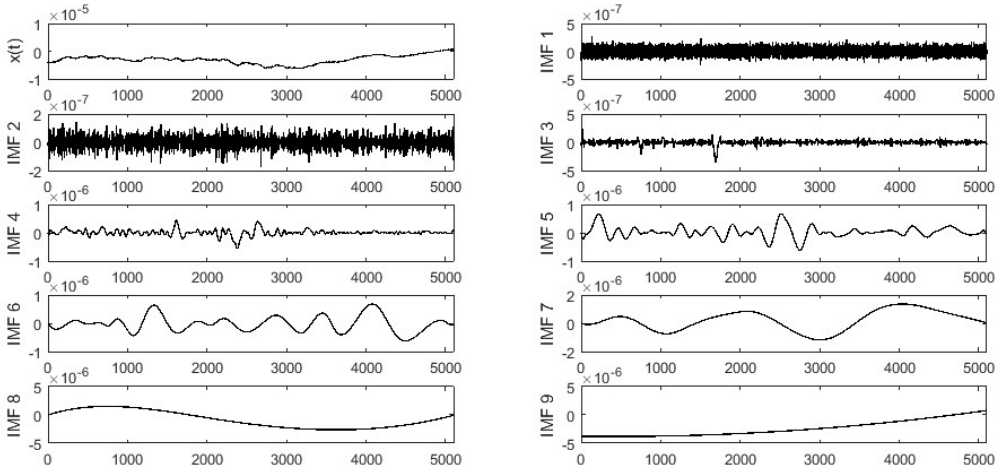

Figure 5. An example of the results of signal $x(t)$ decomposition by the EMD algorithm; the subplots present parts decomposed into 9 IMF components; the trend is estimated by summing up a few of the highest components according to a selected criterion; the OX axes are scaled in seconds [s], the OY axes are scaled in Amperes [A].

2.6 Variational Mode Decomposition

The Variational Mode Decomposition (VMD) was recently proposed by Dragomiretskiy and Zosso [37]. The proposal is an alternative approach to the EMD algorithm [32]. The VMD is a non-recursive method – the modes are extracted concurrently. It decomposes a signal $x(t)$ into a finite number K of compactly band-limited modes $u_k(t)$, called band-limited intrinsic mode functions (BLIMFs). The method is a generalization of the Wiener filter onto multiple and adaptive bands. Therefore, the VMD model is a much more robust treatment of sampling frequency and noise. Thus, the VMD model is suitable for removing or extracting additive noise from nonlinear (generated by the system that does not obey superposition and scaling properties) and nonstationary signals [38].

The basic operating principle of VMD [37] is decomposing a real-valued input signal $x(t)$ into a discrete number of components (modes) u_k, having specific sparsity properties. The sparsity of each mode is its bandwidth in the spectral domain. Each mode is modelled by a sinusoidal signal with a time-varying amplitude A_k and a phase ϕ_k:

$$x(t) = \sum_{k=1}^{K} u_k(t) = \sum_{k=1}^{K} A_k(t) \cos \phi_k(t). \tag{9}$$

We make an assumption that the k-th mode is mostly compact around a central pulsation ω_k, which should be determined in the decomposition stage. In order to determine the bandwidths of the modes the following optimization procedure has been proposed [37]:

1. computation of the associated analytic signal for each mode u_k by means of the Hilbert transform in order to obtain a unilateral frequency spectrum,
2. shifting the frequency spectrum of each mode to a "baseband" by mixing with an exponential tuned to the central frequency estimated respectively,
3. estimation of the bandwidth by the Gaussian smoothness of the demodulated signal, i.e. the squared L^2-norm of the gradient.

The optimization procedure may be represented by the mathematical equation:

$$\min_{\{u_k\},\{\omega_k\}} \left\{ \sum_{k=1}^{K} \left\| \partial_t \left[\left(\delta(t) + \frac{j}{\pi t}\right) * u_k(t) \right] e^{-j\omega_k t} \right\|_2^2 \right\} \text{ subject to } \sum_{k=1}^{K} u_k = x(t), \tag{10}$$

where $\{u_k\}=(u_1,\ldots,u_K\}$ and $\{\omega_k\}=(\omega_1,\ldots, \omega_K\}$ are shorthand notations for the sets of all modes and their central frequencies, respectively. Solving (10) numerically is a relatively complex task and its explanation is beyond the scope of this paper. A detailed description may be found elsewhere [37, 39].

In [40] the authors have presented the use of VMD for a few different tasks, including trend removal. The main assumption is that the trend component is covered by a set of low-frequency BLIMFs. The detrending involves the separation of the low-frequency trend from high-frequency fluctuations. The trend may be directly captured by the evaluated BLIMFs. It may be estimated by summing up the fine-to-coarse components:

$$T_K(t) = \sum_{k=1}^{K} u_k(t). \tag{11}$$

During this task the initial value of the data fidelity constraint parameter (bandwidth parameter) α should be properly chosen. An α value which is too large results in a curve which is too smooth. The choice of the right α value depends on the appropriate anticipation of the meaning of the resulting reconstruction, as was shown elsewhere [40]. The value of α should be kept small, in the range of a few hundred, when we deal with signals containing a very wide range of frequencies (e.g., harmonically distorted signals). An inverse situation is observed for a signal with a smaller range of frequencies (e.g.

detection of flicker, detection of fundamental frequency oscillations), where the α value should be kept very high, in the range of a few tens of thousands. An algorithm of VMD was implemented using MATLAB software (the function *vmd*) and may be applied to noncommercial research [37]. A few parameters have to be set when the above-mentioned MATLAB *vmd* function is used. The first one is a Lagrangian multiplier λ, which enforces an equality constraint of the reconstruction problem (the equation: $\sum_{k=1}^{K} u_k = x(t)$). If an accurate reconstruction is not required, particularly in the presence of either intense noise or a huge trend, the Lagrangian multiplier may be assumed as zero by setting its update parameter $\tau = 0$. The last adjustable parameter of the VMD algorithm is the number *K* of the modes decomposing the input signal. This predefined parameter depends on the number of components comprising the analysed signal and determines the efficiency of the denoising or detrending operation. The number *K* may be selected by checking how much of the spectra of the modes overlap. The *K* value may be either too small (under-binning) or too high (overbinning). A rule of thumb is to use the EMD before using the VMD and to determine *K* based on the number of modes resulting from the EMD method. However, the selection of a real value of *K* is based on experimental knowledge [38].

3. Detrending efficiency assessment

3.1 Histograms of recorded noise

The statistical properties of random data may be evaluated by a histogram – distribution of the recorded data values. The recorded noise usually has a normal (Gaussian) distribution, characterized by its mean value μ and variance σ^2 (or standard deviation σ). The probability density $f(x|\mu, \sigma^2)$ describing the distribution curve is as follows:

$$f(x|\mu, \sigma^2) = \frac{1}{\sqrt{2\sigma^2\pi}} e^{-\frac{(x-\mu)^2}{2\sigma^2}}. \tag{12}$$

To better visualize any deviation of the analysed data distribution from the Gaussian distribution, it may be presented in the form shown in Figure 6. The axis OY is expressed in a logarithmic scale and the axis OX is transformed to a normalized variable *z* given by the equation:

$$z = \frac{x-\mu}{\sigma}. \tag{13}$$

The proposed scaling represents a normal distribution as two straight lines. Thus, any deviation from a normal distribution may easily be detected as a deformation of these straight lines.

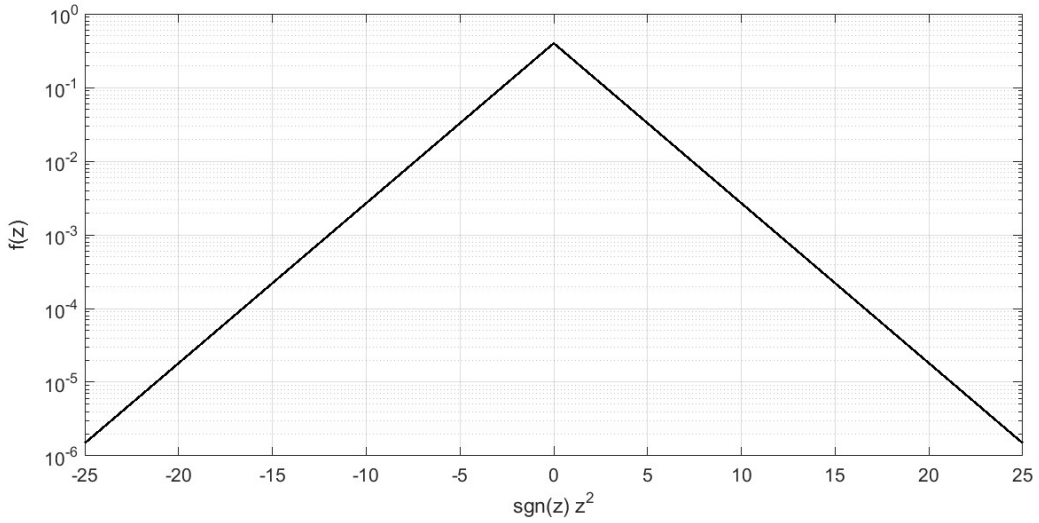

Figure 6. The probability distribution $f(z)$ of a variable z having a standard normal distribution (having zero mean and unit variance values) represented by two straight lines when the axis OY is logarithmic and the axis OX is scaled as $\mathrm{sgn}(z)z^2$; OX and OY units are dimensionless.

In our studies, the estimated histogram was used to detect any non-Gaussian component [41]. We plotted the histogram of a detrended signal after the necessary normalization ($\mu = 0$ and $\sigma^2 = 1$) and compared it with the lines representing a histogram having a standard normal distribution. If the trend component is removed properly, then the residual (detrended) signal should comprise noise having a normal distribution.

We had to limit the random error $\varepsilon_{rh}(x)$ of the histogram estimated around the variable x to compare the estimated values with those of the histogram for a standard normal distribution. The random error $\varepsilon_{rh}(x)$ is given by:

$$\varepsilon_{rh}(x) = \left(\frac{1}{M\Delta x f(x|\mu,\sigma^2)}\right)^{1/2}, \tag{14}$$

where Δx is a range around the variable x where the histogram is estimated, $f(x|\mu, \sigma^2)$ is a probability density function, M is the number of noise samples used for the estimation of the histogram. A more detailed description of histogram estimation and its random error is presented elsewhere [41]. The total number of the recorded noise samples should be approximately a few millions to limit $\varepsilon_{rh}(x)$ to a few percent only when $x = \pm 5\sigma$.

3.2 Power Spectral Density

Another method of evaluating the quality of trend removal is based on the comparison of power spectral densities (PSDs) estimated for the detrended signals by various methods [11, 12, 14]. The power spectral density $S(f)$ of a signal $x(t)$ is estimated by:

$$S(f) = \frac{2}{PT}\sum_{i=1}^{P}|X_i(f)|^2, \tag{15}$$

where: P – the number of averaged spectra, $X_i(f)$ – a Fourier transform of the analysed signal $x(t)$ after multiplying by a selected time window and scaling according to the applied time window to avoid power reduction, T – the observation time of the signal $x(t)$ necessary to determine its Fourier transform $X(f)$. Averaging over P estimated spectra reduces the random error ε_{rp} of $S(f)$, given by:

$$\varepsilon_{rp} = \frac{1}{\sqrt{P}}. \tag{16}$$

We may assess the quality of a trend removal method by comparing the estimated PSD with the assumed PSD of the analysed noise component (e.g., $1/f$ noise). This is the same procedure as in the case of a histogram when we compared the histogram of the signal after the trend removal with a standard normal distribution. Another possible assessment of the trend removal results may be performed by comparing the PSDs estimated for different methods of trend removal. The results show the differences between the considered methods.

3.3 Correlation coefficient

It was proposed in [15] to use a coefficient of linear correlation between the recorded signals after applying a trend removal procedure. In general, a linear correlation coefficient (Pearson correlation coefficient) is a number within the range <-1, 1> assessing a linear correlation between the two considered variables [42, 43]. The Pearson correlation coefficient r_{XY} is a ratio of the covariance $cov(X, Y) = E[(X-E[X])(Y-E[Y])]$, where $E[\ ]$ is an operator of averaging, and the product of standard deviations $\sigma_X \cdot \sigma_Y$ of the analysed random variables X, Y:

$$r_{XY} = \frac{\mathrm{cov}(X,Y)}{\sigma_X \sigma_Y}. \tag{17}$$

The correlation coefficient may compare the applied detrending procedures regarding their efficiency. Effectively removed trends mean that the remnant noise records should be highly correlated. Moreover, a standard deviation within a set of correlation coefficients between noise records, is estimated by applying various procedures, and provides information on the differences between the applied trend removal procedures.

The coefficient r_{XY} is estimated by considering a limited number of the recorded noise samples and therefore we are obliged to apply a statistical test to determine if it is zero or nonzero. The test transforms the coefficient r_{XY}, being a statistical variable, into a new variable $w = 0.5 \cdot \ln\{(1+ r_{XY})/(1- r_{XY})\}$ having a distribution close to the Gaussian one. Then we can test a statistical hypothesis if the coefficient r_{XY} equals zero, as presented in detail elsewhere [43].

3.4 Signal power

Trend removal methods may be compared by estimating the residual powers of signals after the operation of trend removal [17]. The power of the current or voltage random signal (noise) is determined by the physical process generating that noise. Therefore, the signals after trend removal should have similar power values. The power P_S of a discrete signal $x(n)$ consisting of N+1 samples may be estimated by the formula:

$$P_S = \lim_{N\to\infty} \left(\frac{1}{N+1} \sum_{n=0}^{N} |x(n)|^2\right). \tag{18}$$

The estimated P_S should depend on the efficiency of trend removal and therefore may be used to assess the quality of the considered methods. Statistical hypothesis tests, similar to those used for the correlation coefficient [43], may be applied to determine how different the values of P_S are when estimated by a limited number of signal samples.

4. Trend removal using the example of an electrochemical noise time series

4.1 Electrochemical noise generated by the uniform corrosion process

Electrochemical noise is a random signal generated during the electrochemical corrosion processes (e.g. uniform, pitting or crevice corrosion [14]). It may be observed in the form of voltage or current fluctuations between the corroding electrodes at a very low frequency range, up to a few mHz. Therefore, any slow changes of environmental conditions (e.g. slow temperature variations) induce a trend component which has to be removed before analysis of the additive noise component. In our studies we acquired current fluctuations between two corroding electrodes mounted inside a water-supplying pipe [14]. The electrochemical noise measurements were performed in a municipal water supply system. The electrode set was inserted inside one of the parallel 1-inch diameter pipes. The flow of water in the pipe between valves was stopped during electrochemical noise measurements. All electrodes were made from ST3S steel and had a surface area of about 1 cm^2 each. The observed current fluctuations had trends. Current fluctuations were observed in a circuit formed by two identically prepared metal electrodes (named as working electrodes) immersed in municipal water and the electrode terminals that were short circuited by applying a current-voltage converter based on low-noise operational amplifier OPA128. An example of the recorded current $I(t)$ is presented in Figure 7; the data vector consists of 5115 samples collected at a sampling frequency f_s = 1 Hz. The clearly visible drift component may be caused by slow ambient temperature variations and the diffusion of corrosion products during a few hours of data recording or by some unavoidable differences between two identically prepared electrodes. The electrochemical noise generated by uniform corrosion is expected to have a Gaussian distribution and a 1/f-like power spectral density at a low frequency range. We have checked that the power spectrum of the current 1/f noise observed between short circuited corroding electrodes was even two orders more intense than the inherent noise generated by the applied measurement setup. The inherent current noise of the setup was measured at short circuited input of the applied current-voltage converted followed by the National Instruments amplifier SCXI 1121 [14].

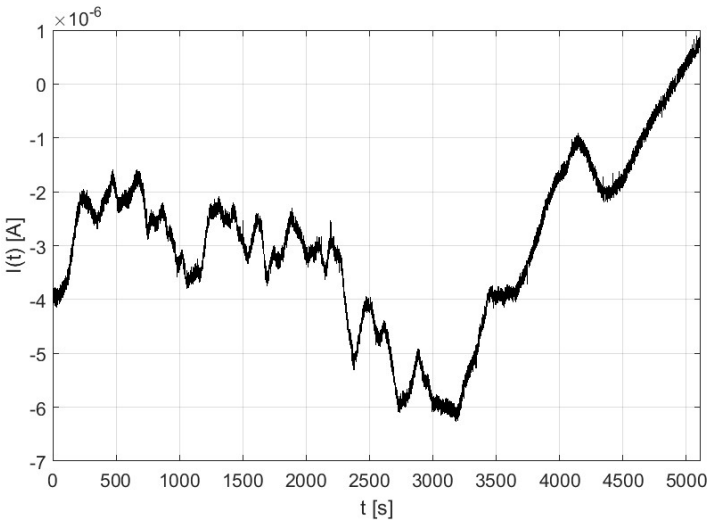

Figure 7. The electrochemical current noise $I(t)$ flowing between two uniformly corroding metal electrodes mounted inside a municipal water pipe.

Figure 8 represents histograms of the data from Figure 7 after applying five considered detrending methods (MAR, polynomial fitting, filtering by wavelet transform, EMD and VMD). The MAR filter parameter was set to p = 7. The polynomial fitting was performed by an approximating polynomial of

the 21st order. Filtering by the wavelet transform was accomplished by applying a 4-th order Daubechies wavelet function and by decomposing the signal to the eighth level. The EMD method decomposed the time series into nine IMFs. The first five IMFs were selected by using the energy-ratio approach [35] to determine the detrended signal. The VMD applied the MATLAB *vmd* function; the parameter values $\alpha = 9 \cdot 10^6$ and $\tau = 0$ were chosen to remove the trend in a most effective way.

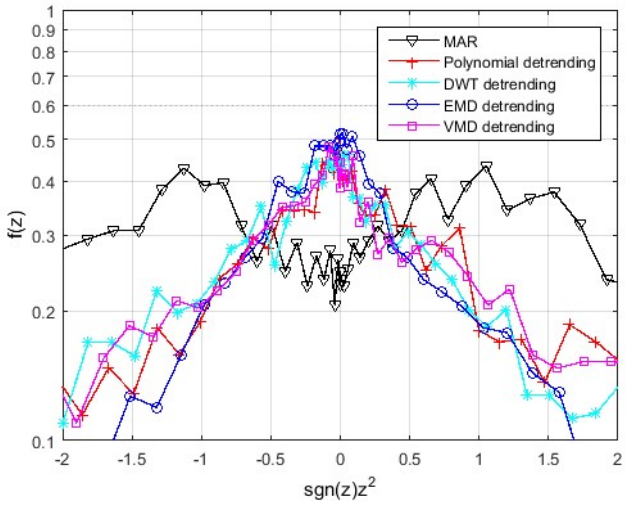

Figure 8. Probability distribution $f(z)$ of the detrended electrochemical current noise $I(t)$ (Figure 7) after applying the trend removal procedures: MAR filtering, polynomial approximation, DWT filtering, EMD and VMD; OX and OY units are dimensionless.

Four detrending methods identified the trend relatively well (Figure 8). Application of the MAR filtering method resulted in a histogram differing from a Gaussian distribution more than the histograms obtained with the other methods considered. The power spectra were quite similar to each other except for the spectrum obtained with the MAR method (Figure 9). This spectrum was attenuated at a low frequency range according to its filter transfer function (Figure 2). The power spectral density of the original signal with a visible trend component was about 25% more intense at a low frequency range than the power spectra estimated after trend removal by polynomial, EMD or VMD detrending (Figure 9). We would like to emphasize that the popular and simple method of polynomial detrending may produce reasonable results but require the selection of the appropriate order of the applied polynomial and therefore its simplicity may be misleading when compared with other more advanced methods however, it is performed automatically. When a detrending operation is limited to e.g., a linear trend removal function, the results may became unacceptable.

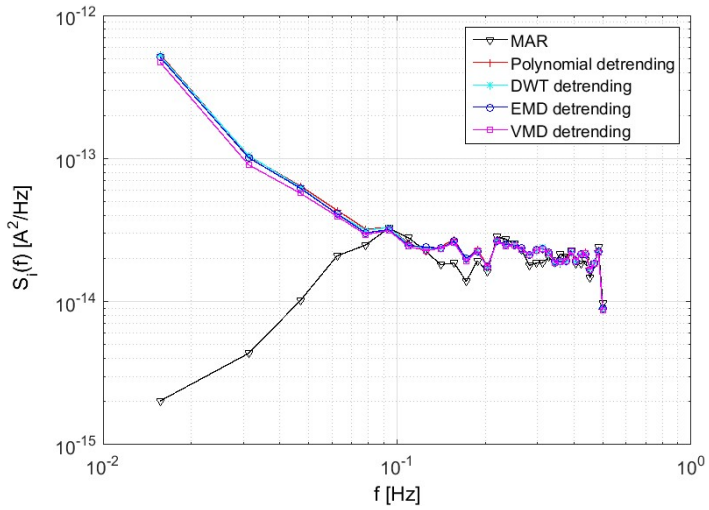

Figure 9. Power spectral densities $S_i(f)$ of the detrended electrochemical noise (current fluctuations) time records (Figure 7) obtained with different trend removal methods; power spectral densities were estimated by using 128 samples and averaged over 40 spectra.

Table 1 presents linear correlation coefficients estimated for the signals when the trend component was removed with one of the presented methods. It confirms again that all methods except for MAR filtering determine closely correlated detrended signals ($r_{XY} \approx 0.7$-0.9). These results confirm that the four considered methods (polynomial fitting, filtering by wavelet transform, EMD and VMD) may be effectively applied to the recorded electrochemical noise data for trend removal.

Table 1. Linear correlation coefficients r_{XY} estimated when the electrochemical noise (Figure 7) was detrended with the methods considered.

r_{XY}	**MAR**	**Polynomial**	**DWT**	**EMD**	**VMD**
MAR	1	0.3671	0.3942	0.3761	0.4126
Polynomial	0.3671	1	0.8286	0.7530	0.9017
DWT	0.3942	0.8286	1	0.8856	0.9096
EMD	0.3761	0.7530	0.8856	1	0.8844
VMD	0.4126	0.9017	0.9096	0.8844	1

A similar conclusion may be drawn from the estimated signal powers P_S for the detrended signals (Table 2). The estimated P_S value was only far different for the MAR method. The other methods considered produced quite similar results.

The presented results were obtained for relatively short time records (128 x 40 = 5120 samples). This is due to a low sampling frequency and a limited period of data recording. It determined the frequency resolution of the estimated power spectral density. We may conclude that a longer data sampling period would secure a better frequency resolution and limit the spectral leakage. The estimated power spectral densities are therefore deformed due to the limited observation period and the assumed frequency resolution. The considered data represent a common case of electrochemical noise data analysis with existing constrains.

Table 2. Signal power P_S values of the electrochemical noise (Figure 7) after detrending with the methods considered.

	MAR	Polynomial	DWT	EMD	VMD
$P_S \cdot 10^{-14}$	0.98	7.99	6.93	7.79	6.33

4.2 Electrochemical noise generated during the discharging of supercapacitors

The second data set for the examination of the detrending methods was acquired during the accelerated ageing of experimental specimens of supercapacitors [44]. The considered specimens (capacitance of about 3 F, electrolyte: 1 mol L^{-1} TEA BF_4, electrodes: BATSCAP about 110 µm, separator: cellulose 35 µm, aluminium foil 30 µm) were aged by floating (a constant value of voltage attached to the supercapacitor terminals during a given period of ageing) or cycling (numerous charging/discharging events using relatively high currents). The state of an aged specimen was determined by measuring the noise component during slow discharging through a 1 kΩ resistor. Low frequency noise was generated within porous carbon electrodes of the investigated supercapacitor by charge redistribution or eventual redox reactions induced by excessive voltage when aged by floating. Similar method was proposed to determine a state of health of commercial Li-ion batteries [45].

Discharging current (with its noise component) flowing through the above-mentioned loading resistor was observed as a voltage drop between the terminals of the loading resistor by the attached data acquisition board (National Instruments NI 4431). An example of the discharging current $I_d(t)$ waveform is presented in Figure 10. The data vector consists of 7 864 321 samples collected at a sampling frequency f_s = 1024 Hz. The trend component is so large that it hides the random component, enlarged in the inset in Figure 10 for better visualization. This random component is expected to have a Gaussian distribution. The trend component can't be approximated by an exponential decay function because the approximation is not sufficiently precise and the results are unsatisfactory to identify noise component. The supercapacitor has to be modeled by a set of RC elements (resistors R and capacitors C), connected in a parallel way [44, 45]. Additionally, some of these RC components may depend on the applied charging voltage and may change during the discharging process.

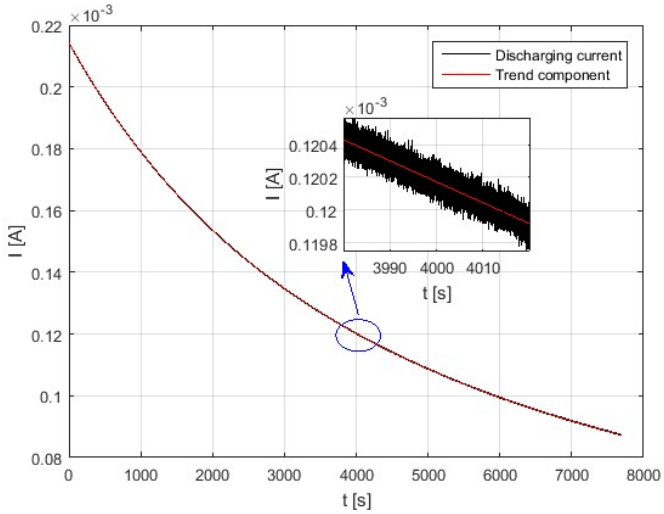

Figure 10. The discharging current of a supercapacitor with an inset visualizing its random component.

The observed noise component during supercapacitor discharge is generated within its structure because the current power spectral density of the inherent noise of the applied measurement setup

was at least ten times lower at a frequency range below 1 Hz than the power spectrum estimated during the discharging process. The inherent noise of the measurement setup was measured in the same circuit when the loading resistor and the discharged supercapacitor were only connected to the input of an analog-digital converter.

Our numerous experimental studies have confirmed that the recorded noise is intensified by the aging processes of the supercapacitor, when the specimen was polarized by a relatively high DC voltage [46]. The power spectral density of the current fluctuations during discharging even increased a few times shortly before a drop of capacitance in numerous experiments. We have observed during an investigation of the disassembled specimen some small crevices and local delamination of carbon layer from the metal collector on a positive capacitor electrode mainly. These effects are induced by the corrosion processes taking place at the surface of metal collector or in the pores of carbon electrodes as reported elsewhere [48–50]. Corrosion products which have a greater volume would result in the cracking of the fragile carbon layer and its local delamination. Noise intensifies when corrosion processes escalate at higher polarizing voltages during aging and therefore the determination of the noise component may be used to monitor the quality of the tested supercapacitor.

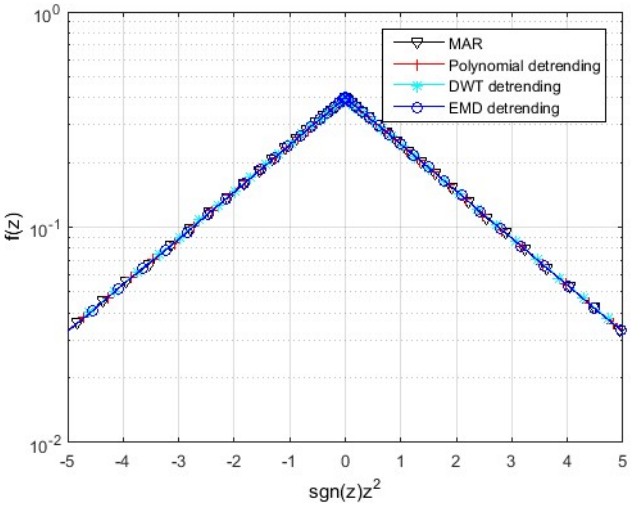

Figure 11. The probability distribution $f(z)$ of the detrended signals obtained with different trend removal methods using the discharging currents of supercapacitor specimens; OX and OY units are dimensionless.

Figure 11 presents histograms obtained after the detrending processes performed by four of the above-mentioned methods (MAR, polynomial fitting, wavelet and EMD). The MAR filter parameter was set to $p = 7$, whereas the polynomial fitting was accomplished with a 6^{th}-order polynomial. The selected polynomial order is a compromise between flexibility of trend approximation by polynomial and possible appearance of undesirable ripples when a too high polynomial order was selected. This order was established by practical experience, considering the results of numerous electrochemical noise data analyses. The wavelet detrending used a 4^{th}-order Daubechies wavelet and eighteen levels of decomposition. The EMD decomposed the examined time series into eleven IMFs. The first nine of them were selected (using the energy-ratio approach [35]) to reconstruct the signal with the trend component filtered out. The VMD method could not be used because the analysed time series were very long (about 8 million samples, in the case of homogenous corrosion it was only about 5 thousand samples) and the memory volume required for the necessary computations was much higher than that of our PC.

It is clear from Figure 11 that almost all of the explored detrending methods resulted in a relatively good elimination of the trend component. All histograms proved that the noise component distribution was close to a normal distribution. Power spectral densities of the detrended signals (Figure 12) proved the effectiveness of the considered methods with the exception of the MAR filtering method. The PSD of the detrended signal obtained with MAR filtering is different from all other spectra due to its filter transfer function (Figure 2). Some deviation of the PSD at a low frequency range was also observed for the signal detrended by the EMD algorithm.

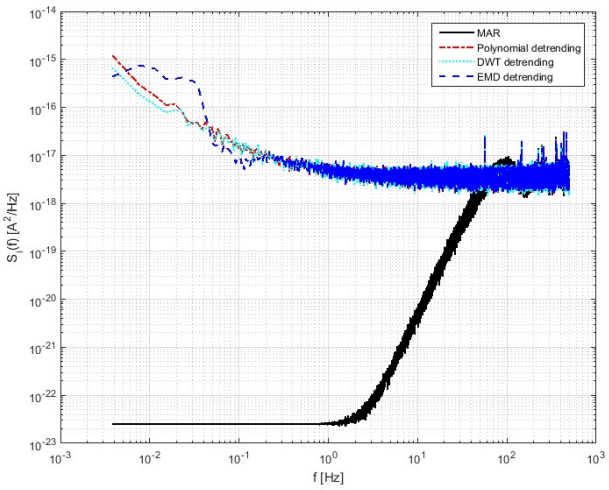

Figure 12. Power spectral densities $S_i(f)$ of the detrended signals (current fluctuations) obtained with different trend removal methods from the current observed during supercapacitor discharging through a 1 kΩ resistor.

Table 3 presents the correlation coefficients estimated for the signals after the trend removal using all of the methods considered with the exception of the VMD algorithm. It is clear that - except for the MAR filtering – the other methods are closely correlated ($r_{XY} \approx 1$). The results proved the effectiveness of detrending with the polynomial fitting, wavelet transform and EMD algorithms.

Table 3. Correlation coefficients r_{XY} determined for the signals detrended using selected methods.

r_{XY}	MAR	Polynomial	DWT	EMD
MAR	1	0.96	0.96	0.97
Polynomial	0.96	1	0.99	0.99
DWT	0.96	0.99	1	0.99
EMD	0.97	0.99	0.99	1

Table 4 shows the estimated power P_S values of the signals after the removal of the trend component using the methods considered. It is clear that - except for the MAR filtering - all other methods produced very similar results. The EMD method resulted in some undulations at a low frequency range (Figure 12). That means that this method has some limitations regarding the considered current records and therefore other algorithms (even those requiring less computing power, e.g. the polynomial approximation) should be applied.

Table 4. Power P_S values of the detrended signals.

	MAR	Polynomial	DWT	EMD
$P \cdot 10^{-15}$	1.80	1.94	1.93	1.93

5. Conclusions

In our exploratory studies a few trend removal methods have been presented. With the exception of MAR filtering, the other methods which were evaluated may be successfully used for electrochemical noise data processing but they exhibit some visible differences in efficiency of trend removal. Better results were achieved for trend removal of the data observed during discharging of supercapacitor than those generated by corrosion processes. This conclusion means that the same methods for longer time records and for a trend being a smooth function give better results.

We may conclude that the appropriate choice of a method and its parameters are closely dependent on the trend form. For the trends consisting of oscillatory components, the DWT, EMD or VMD algorithms should be preferred. These methods (e.g., DWT, EMD or VMD) utilize oscillatory functions to determine conformity between the analysed signal and the applied characteristic functions in the enumerated methods (e.g., convolution of the input signal with different wavelet functions for DWT), and therefore are expected to give better results. In general, we recommend the application of the proposed methods to assess the quality of detrending algorithms by comparing either the power spectra of signals detrended by various methods or other estimated statistical parameters (e.g. correlation coefficient r_{XY}, power P_S or histogram if possible) of these signals. Such a procedure enables to assess the efficiency of a trend removal method for any trend and analysed time records of any length. The main conclusion of the review is that the proposed procedure of trend removal and assessing its efficiency by the mentioned statistical parameters is a universal one and may be applied for any type of trend. By considering selected statistical parameters a more rational assessment of the presented methods may be performed to secure the best possible selection. The set of considered trend removal methods is so wide that we should be able to select an appropriate method to produce decent results for any experimental data of electrochemical noise as considered in numerous papers published within the last few years [10, 15, 52].

Acknowledgements

This work was supported by the National Science Centre, Poland, the grant decision: DEC-2014/15/B/ST4/04957 “Charging/discharging mechanism at the electrode/electrolyte interface of supercapacitors”.

Conflicts of Interest

The authors declare that they have no conflict of interest.

Bibliography

[1] K.H. Chan, J.C. Hayya, J.K. Ord, A Note on Trend Removal Methods: The Case of Polynomial Regression versus Variate Differencing, Source Econom. 45 (1977) 737–744. doi:10.2307/1911686.

[2] L.M. Vicente, A.B. Barreto, A. Taberner, Adaptive pre-processing of photoplethysmographic blood volume pulse measurements, in: Proc. 1996 Fifteenth South. Biomed. Eng. Conf., IEEE, n.d.: pp. 114–117. doi:10.1109/SBEC.1996.493126.

[3] A. van der Ziel, Flicker Noise in Electronic Devices, Adv. Electron. Electron Phys. 49 (1979) 14649.

[4] Ł. Lentka, J.M. Smulko, R. Ionescu, C.G. Granqvist, L.B. Kish, Determination of gas mixture components using fluctuation enhanced sensing and the LS-SVM regression algorithm, Metrol. Meas. Syst. 22 (2015) 341–350. doi:10.1515/mms-2015-0039.

[5] M. Kiwilszo, J. Smulko, Pitting corrosion characterization by electrochemical noise measurements on asymmetric electrodes, J. Solid State Electrochem. 13 (2008) 1681–1686. doi:10.1007/s10008-008-0643-y.

[6] L. Kristoufek, Detrending moving-average cross-correlation coefficient : Measuring cross-correlations between non-stationary series, Physica A. 406 (2014) 169–175. doi:10.1016/j.physa.2014.03.015.

[7] P. Brockwell, R. Davis, Introduction to Time Series and Forecasting, 2002. doi:10.2307/1271510.

[8] T. Alexandrov, S. Bianconcini, E. Dagum, A review of some modern approaches to the problem of trend extraction, Econometric. (2012).

[9] X. Deng, D. Yang, J. Peng, X. Guan, B. Yang, Noise reduction and drift removal using least-squares support vector regression with the implicit bias term, Geophysics. (2010). doi:10.1190/1.3506602.

[10] Xia, D. H., Song, S. Z., & Behnamian, Y. Detection of corrosion degradation using electrochemical noise (EN): review of signal processing methods for identifying corrosion forms, Corrosion Engineering, Science and Technology 51 (2016) 527–544.

[11] U. Bertocci, F. Huet, R.P. Nogueira, P. Rousseau, Drift removal procedures in the analysis of electrochemical noise, Corrosion. 58 (2002) 337–347. doi:10.5006/1.3287684. [12] F. Mansfeld, Z. Sun, C.H. Hsu, A. Nagiub, Concerning trend removal in electrochemical noise measurements, Corros. Sci. 43 (2001) 341–352. doi:10.1016/S0010-938X(00)00064-0.

[12] F. Mansfeld, Z. Sun, C.H. Hsu, A. Nagiub, Concerning trend removal in electrochemical noise measurements, Corros. Sci. 43 (2001) 341–352. doi:10.1016/S0010-938X(00)00064-0.

[13] Y.J. Tan, S. Bailey, B. Kinsella, The monitoring of the formation and destruction of corrosion inhibitor films using electrochemical noise analysis (ENA), Corros. Sci. 38 (1996) 1681–1695. doi:10.1016/S0010-938X(96)00061-3.

[14] J.M. Smulko, K. Darowicki, A. Zielinski, On Electrochemical Noise Analysis for Monitoring of Uniform Corrosion Rate, IEEE Trans. Instrum. Meas. 56 (2007) 2018–2023. doi:10.1109/TIM.2007.895624.

[15] A.M. Homborg, T. Tinga, X. Zhang, E.P.M. Van Westing, P.J. Oonincx, J.H.W. De Wit, J.M.C. Mol, Time-frequency methods for trend removal in electrochemical noise data, Electrochim. Acta. 70 (2012) 199–209. doi:10.1016/j.electacta.2012.03.062.

[16] R. Maizia, A. Dib, A. Thomas, S. Martemianov, Proton exchange membrane fuel cell diagnosis by spectral characterization of the electrochemical noise, Journal of Power Sources. 342 (2017) 553–561.

[17] S.Z. Song, W.X. Zhao, J.H. Wang, J. Li, Z.M. Gao, D.H. Xia, Field Corrosion Detection of Nuclear Materials using Electrochemical Noise Technique, Protection of Metals and Physical Chemistry of Surfaces. 54 (2018) 340–346.

[18] D.H. Xia, Y. Behnamian, Electrochemical noise: a review of experimental setup, instrumentation and DC removal. Russian Journal of Electrochemistry, 51(7) (2015) 593–601.

[19] C. Ma, S. Song, Z. Gao, J. Wang, W. Hu, Y. Behnamian, D.H. Xia, Electrochemical noise monitoring of the atmospheric corrosion of steels: identifying corrosion form using wavelet analysis, Corrosion Engineering, Science and Technology. 52 (2017) 432–440.

[20] J.W. Demmel, Applied numerical linear algebra, (2008).

[21] I.T. Jolliffe, A Note on the Use of Principal Components in Regression, J. R. Stat. Soc. Ser. C (Applied Stat. 31 (1982) 300–303. doi:10.2307/2348005.

[22] O. Scepanovic, K. Bechtel, A. Haka, W. Shih, T. Koo, A. Berger, M. Feld, Determination of uncertainty in parameters extracted from single spectroscopic measurements, J. Biomed. Opt. 12 (2007) 64012. doi:10.1117/1.2815692.

[23] I. Barman, N.C. Dingari, G.P. Singh, J.S. Soares, R.R. Dasari, J.M. Smulko, Investigation of noise-induced instabilities in quantitative biological spectroscopy and its implications for noninvasive glucose monitoring., Anal. Chem. 84 (2012) 8149–56. doi:10.1021/ac301200n.

[24] C. Vamoş, Automatic algorithm for monotone trend removal, Phys. Rev. E - Stat. Nonlinear, Soft Matter Phys. 75 (2007). doi:10.1103/PhysRevE.75.036705.

[25] R. Cottis, A. Homborg, J. Mol, The relationship between spectral and wavelet techniques for noise analysis, Electrochim. Acta. 202 (2016) 277–287. doi:10.1016/j.electacta.2015.11.148.

[26] S.G. Mallat, A Theory for Multiresolution Signal Decomposition: The Wavelet Representation, IEEE Trans. Pattern Anal. Mach. Intell. 11 (1989) 674–693. doi:10.1109/34.192463.

[27] J. Smulko, K. Darowicki, A. Zieliński, Pitting corrosion in steel and electrochemical noise intensity, Electrochem. Commun. 4 (2002) 388–391. doi:10.1016/S1388-2481(02)00317-X.

[28] D.L. Donoho, I.M. Johnstone, Ideal Denoising in an orthonormal basis chosen from a library of bases, Comptes Rendus Acad. Sci., Ser. I. 319 (1994) 1317–1322.

[29] M. Misiti, Y. Misiti, Wavelet toolbox, MathWorks Inc. (1996).

[30] M.G. Astaf'ev, L.S. Kanevskii, B.M. Grafov, Analyzing Electrochemical Noise with Chebyshev's Discrete Polynomials, Russ. J. Electrochem. 43 (2007) 17–24.

[31] B. Grafov, Y.A. Dobrovol'skii, A.D. Davydov, A.E. Ukshe, A.L. Klyuev, E.A. Astaf'ev, Electrochemical Noise Diagnostics: Analysis of Algorithm of Orthogonal Expansions, Russ. J. Electrochem. 51 (2015) 503–507.

[32] N.E. Huang, Z. Shen, S.R. Long, M.C. Wu, H.H. Shih, Q. Zheng, N.-C. Yen, C.C. Tung, H.H. Liu, The empirical mode decomposition and the {H}ilbert spectrum for nonlinear and non-stationary time series analysis, Proc. R. Soc. Lond. A 495 (1998) 903–995.

[33] G. Rilling, P. Flandrin, P. Es, On empirical mode decomposition and its algorithms, in: IEEE-EURASIP Work. Nonlinear Signal Image Process., 2003: pp. 8–11. doi:10.1109/ICASSP.2008.4518437.

[34] P. Flandrin, P. Es, G. Rilling, Detrending and denoising with empirical mode decompositions, in: Signal Process. Conf. 12th Eur. IEEE, 2004: pp. 1581–1584.

[35] A. Moghtaderi, P. Flandrin, P. Borgnat, Trend filtering via empirical mode decompositions, Comput. Stat. Data Anal. 58 (2013) 114–126. doi:10.1016/j.csda.2011.05.015.

[36] Z. Yang, B.W.K. Ling, C. Bingham, Trend extraction based on separations of consecutive empirical mode decomposition components in Hilbert marginal spectrum, Meas. J. Int. Meas. Confed. 46 (2013) 2481–2491. doi:10.1016/j.measurement.2013.04.071.

[37] K. Dragomiretskiy, D. Zosso, Two-Dimensional Variational Mode Decomposition_, IEEE Trans. Signal Process. 62 (2014) 531–544. doi:10.1109/TSP.2013.2288675.

[38] Y. Liu, G. Yang, M. Li, H. Yin, Variational mode decomposition denoising combined the detrended fluctuation analysis, Signal Processing. 125 (2016) 349–364. doi:10.1016/j.sigpro.2016.02.011.

[39] S. Samantaray, P. ACHLERKAR, M.S. Manikandan, Variational Mode Decomposition and Decision Tree Based Detection and Classification of PowerQuality Disturbances in Grid-Connected Distributed Generation System, IEEE Trans. Smart Grid. (2016) 1–1. doi:10.1109/TSG.2016.2626469.

[40] Y. Wang, R. Markert, Filter bank property of variational mode decomposition and its applications, Signal Processing. 120 (2016) 509–521. doi:10.1016/j.sigpro.2015.09.041.

[41] J. Smulko, C.-G. Granqvist, L.B. Kish, on the Statistical Analysis of Noise in Chemical Sensors and Its Application for Sensing, Fluct. Noise Lett. 1 (2001) L147–L153. doi:10.1142/S0219477501000366.

[42] J. Benesty, J. Chen, Y. Huang, On the importance of the pearson correlation coefficient in noise reduction, IEEE Trans. Audio, Speech Lang. Process. 16 (2008) 757–765. doi:10.1109/TASL.2008.919072.

[43] J.S. Bendat, A. Piersol, Random Data; Analysis and Measurement Procedures, 2010.

[44] R. Faranda, A new parameters identification procedure for simplified double layer capacitor two-branch model, Electric Power Systems Research. 80 (2010) 363–371.

[45] V. Sedlakova, J. Sikula, J. Majzner, P. Sedlak, T. Kuparowitz, B. Buergler, P. Vasina, Supercapacitor equivalent electrical circuit model based on charges redistribution by diffusion, Journal of Power Sources 286 (2015) 58–65.

[46] A. Szewczyk, Ł. Lentka, J. Smulko, P. Babuchowska, F. Beguin, Measurements of flicker noise in supercapacitor cells, in: 24th Int. Conf. Noise Fluctuations, ICNF, Vilnius, Lithuania, 2017.

[47] S. Martemianov, N. Adiutantov, Y. K. Evdokimov, L. Madier, F. Maillard, A. Thomas, New methodology of electrochemical noise analysis and applications for commercial Li-ion batteries. Journal of Solid State Electrochemistry, 19 (2015) 2803-2810.

[48] M. He, K. Fic, E. Fra, P. Novák, E. J. Berg, Ageing phenomena in high-voltage aqueous supercapacitors investigated by in situ gas analysis. Energy & Environmental Science, 9(2), (2016) 623–633.

[49] K. Kopczyński, G. Milczarek, G. Lota, Polysulphides reversible faradaic reactions in supercapacitor application. Electrochemistry Communications, 68 (2016) 28–31.

[50] P. Ratajczak, K. Jurewicz, F. Béguin, Factors contributing to ageing of high voltage carbon/carbon supercapacitors in salt aqueous electrolyte. Journal of Applied Electrochemistry, 44(4) (2014) 475–480.

[51] R. A. Cottis, Interpretation of electrochemical noise data. Corrosion, 57(3) (2001) 265–285.

[52] A. Ehsani, M. G. Mahjani, M. Hosseini, R. Safari, R. Moshrefi, H. M. Shiri, Evaluation of Thymus vulgaris plant extract as an eco-friendly corrosion inhibitor for stainless steel 304 in acidic solution by means of electrochemical impedance spectroscopy, electrochemical noise analysis and density functional theory. Journal of colloid and interface science, 490 (2017) 444–451.